Long Term Vortex Flow Evolution around a Magnetic Island in Tokamaks

G. J. Choi[*] and T. S. Hahm

Department of Nuclear Engineering, Seoul National University, Seoul 151-742, Korea

We present a gyrokinetic analysis of the vortex flow evolution in a magnetic island in collisionless tokamak plasmas. In a short term $\bar{\omega}_D t < 1$, where $\bar{\omega}_D$ is the secular magnetic drift of the orbit center, initial monopolar vortex flow approaches to its residual level determined by the neoclassical enhancement of polarization shielding after collisionless relaxation. The residual level depends on the location inside an island and is higher than the Rosenbluth-Hinton level [M.N. Rosenbluth and F.L. Hinton, Phys. Rev. Lett. **80**, 724 (1998)] due to finite island width. In a long term $\bar{\omega}_D t > 1$, the residual vortex flow evolves to a dipolar zonal-vortex flow mixture due to toroidicity-induced breaking of a helical symmetry. The mixture forms localized flow shear layers near the island separatrix away from X points. The deviation of the streamlines of the mixture flows from magnetic surfaces allows turbulence advection across the island. We expect a small island $w \lesssim q\rho_{Ti}/\hat{s}$ provides a favorable condition for this mixture flow formation, while the monopolar vortex flow persists for a larger island.

In the magnetic fusion community, there has been growing interest in magnetic islands (MIs) interactions [1–3] with microturbulence for thorough understanding and prediction of confinement of magnetized fusion plasmas. In fusion plasmas, MIs are often generated by intrinsic tearing instabilities [4] or external perturbations [5,6] accompanying a magnetic reconnection which is also an outstanding research subject in astrophysical context. Their impact on the confinement has turned out to be more complicated than simple degradation by parallel collisional transport. For example, MI formation at the H-mode pedestal top can be crucial [7] for the resonant magnetic perturbation-induced suppression of edge-localized modes [8], leading to a sustainable H-mode operation. Moreover, MIs can sometimes induce confinement enhancement [9] accompanied by an internal transport barrier formation. Its leading physics mechanism is reduction of turbulent transport by E × B flow shear [10,11]. In an MI, measurements suggest that E × B shear flows circulate on the island contours [12,13], forming monopolar vortex flows.

In addition, simulation studies [14–17] have found self-generation of the vortex flows from turbulence, with a simultaneous regulation of the turbulence level by the vortex flow shearing. This is reminiscent of self-regulation of turbulence by zonal flows which has been extensively studied previously [18–20]. The turbulence-driven zonal flows streaming on the nested magnetic surfaces is a prime example of the self-organization in magnetized plasmas [21,22]. While this common feature of the zonal and vortex flows has promoted experimental [2,3,23] and simulation studies [1,14–17,24] of the flow dynamics in MIs, there still has been a lack of analytic progress on the vortex flows. Rare exceptions include a pioneering work on the vortex

flow generation [25] based on the wave kinetics in the reduced MHD system, and a recent work identifying highly anisotropic vortex flow shearing rate around an MI [26]. Alongside the generation and the shearing, understanding the damping process of turbulence-driven flows is an important issue [27], as it is directly related with the saturated turbulence level which limits the plasma performance. Nevertheless, there has been no analytic work on this issue for the vortex flows.

In this Letter, we present an analytic theory of the vortex flow evolution in an MI in collisionless tokamak plasmas for the first time, based on the nonlinear gyrokinetics [28–30]. We find that the vortex flow evolution in MIs shows a distinct feature from that of the zonal flows in tokamaks. The residual monopolar vortex flows which survive after the transit-time magnetic pumping naturally evolve in a longer term to a dipolar flow with a considerable axisymmetric zonal component near the X point. This leads to localized flow shear layers near the island separatrix away from the X point. In addition, consequent deviation of the contours of the streamlines from those of the magnetic surfaces opens a route for turbulence to be advected through a region near the X point into the MI.

In tokamak plasmas, a MI at the mode rational surface is represented by the perturbed poloidal magnetic flux $\delta\psi = \tilde{\psi}\cos(m\alpha)$, where the amplitude $\tilde{\psi}$ is considered to be a constant around the MI [31]. Here, $\alpha = \theta - \zeta/q_s$ is the helical angle, where $q_s = m/n$ is the safety factor at the rational surface, and m and n are poloidal and toroidal mode numbers of the island. We consider a static MI without addressing the MI dynamics of the tearing mode [32]. As such, we assume that the vortex flow evolution occurs in a timescale shorter than the resistive diffusion

time characterizing the MI growth in the Rutherford regime [31]. We consider a circular-concentric low-β tokamak plasma without Shafranov shift and use the orthogonal toroidal coordinates (r, θ, ζ), where r is the radial distance from the magnetic axis and θ and ζ are the poloidal and the toroidal angles. In the vicinity of the MI, the proper label for the magnetic surfaces is the helical magnetic flux $\psi_h = \psi - \chi/q_s$ [33], where ψ and χ are the total poloidal and toroidal magnetic fluxes. We use a normalized helical magnetic flux [31]

$$X = -\frac{\psi_h}{\tilde{\psi}} = 2\frac{x^2}{w^2} - \cos(m\alpha). \qquad (1)$$

Here, $x = r - r_s$ is the radial distance from the mode rational surface r_s, and w is half-width of the MI given by $w^2 = 4(r_s L_s/m)(\tilde{B}_r/B)$, where $\tilde{B}_r = m\tilde{\psi}/r_s R$ is the amplitude of the perturbed magnetic field and $L_s = qR/\hat{s}$. Inside the MI, we have $X \in [-1, 1]$, where $X = -1$ at the O point and $X = 1$ at the island separatrix. Equation (1) defines the island geometry which has a helical symmetry, i.e., an invariance under a translation along the reference helical magnetic field line $\mathbf{B}_s$. Within this model, the in-out asymmetry of MI due to toroidicity is absent. Extension to a simple model stellarator equilibrium is possible with an appropriate choice of flux functions.

For the electrostatic potential representing the E × B vortex flows, we apply the eikonal representation

$$\delta\phi = \phi(\mathbf{R}, t) \exp\{iS(X)\}, \qquad (2)$$

where the eikonal function $S(X)$ captures the fast variation across the island flux surface and the envelope $\phi(\mathbf{R}, t)$ describes the rest. Here, $\mathbf{R}$ is the gyrocenter position. Similarly, we use $\delta g = g \exp(iS)$, where δg is the gyrophase angle-independent part of the nonadiabatic response of the particle distribution function satisfying $\delta f = -(e\delta\phi/T)F_0 + \delta g \exp(-i\mathbf{k} \cdot \boldsymbol{\rho})$. Here, F_0 is the equilibrium distribution function, $\mathbf{k} = \nabla S$ is the vortex flow wave vector and $\boldsymbol{\rho}$ is the gyroradius vector. The gyrokinetic equation for the vortex flows is

$$\frac{\partial g}{\partial t} + v_\| \mathbf{b} \cdot \nabla g + i\omega_D g + \mathbf{v}_d \cdot \nabla g = \frac{e}{T}F_0 J_0 \frac{\partial\phi}{\partial t} + NF_0, \qquad (3)$$

where $\mathbf{b}$ is a unit vector along the total magnetic field, $\mathbf{v}_d$ is the magnetic drift velocity, $\omega_D \equiv \mathbf{k} \cdot \mathbf{v}_d$ is the magnetic drift frequency, $J_0 = J_0(k_X\rho)$ is a Bessel function, $k_X \equiv |\mathbf{k}|$, and NF_0 is the vortex flow source from the E × B nonlinearity. The third and fourth terms on the left-hand side (LHS) represent the eikonal factor and envelope contributions to the magnetic drift of δg. While the latter is small compared to the former, it is an essential piece in the long term evolution of the vortex flows which will be shown later. The magnetic drift frequency can be written as [34]

$$\omega_D = v_\| \mathbf{b} \cdot \nabla Q + \bar{\omega}_D, \qquad (4)$$

where Q is the finite orbit width (FOW) factor and $\bar{\omega}_D$ is the secular drift frequency of the orbit center. Here, the bounce-average $\overline{(\cdots)} \equiv [\oint dl_\|(\cdots)/v_\|]/(\oint dl_\|/v_\|)$ eliminates dynamics faster than or comparable to the bounce or transit motion. For the evolution of the vortex flows after fast collisionless relaxation, we multiply Eq. (3) by $\exp(iQ)$ and take the bounce average to obtain the bounce-averaged kinetic equation

$$\frac{\partial h}{\partial t} + \overline{e^{iQ}\mathbf{v}_d \cdot \nabla(he^{-iQ})} + i\bar{\omega}_D h$$
$$= \frac{e}{T}F_0\frac{\partial}{\partial t}\overline{e^{iQ}J_0\phi} + \overline{e^{iQ}N}F_0, \qquad (5)$$

where $h = \overline{g\exp(iQ)}$ is the bounce-angle-independent part of g for $t > \omega_b^{-1}$. The LHS of Eq. (5) can be simplified as follows in the long-wavelength limit $k_X\rho \ll Q \ll 1$,

$$\frac{\partial h}{\partial t} + \omega_{\mathrm{pr}}\frac{\partial h}{\partial\zeta}\Big|_\psi + i\bar{\omega}_D h = \frac{e}{T}F_0\frac{\partial}{\partial t}\overline{e^{iQ}J_0\phi} + \overline{e^{iQ}N}F_0. \qquad (6)$$

Here, $\omega_{\mathrm{pr}} = \overline{\mathbf{v}_d \cdot \nabla\zeta}$ is the toroidal precession frequency. Note that the origin of $\bar{\omega}_D$, the secular drift frequency across the island magnetic surface X, is also the toroidal precession, because $\bar{\omega}_D \propto \overline{\mathbf{v}_d \cdot \nabla\alpha} \propto \overline{\mathbf{v}_d \cdot \nabla\zeta}$. With $1 < q \sim k_X w$, we have $\bar{\omega}_D \sim \omega_{\mathrm{pr}}$.

Short term evolution.—Fully consistent nonlinear gyrokinetic calculation of the vortex flow is a formidable task. Here we pose the problem following [27] in which NF_0 in Eq. (3) from the E × B nonlinearity is modeled by an initial kick acting as the unit flow source. We first consider the vortex flows in a short term $\omega_b^{-1} < t < \omega_{\mathrm{pr}}^{-1}$, neglecting the second and the third terms on the lhs of Eq. (6). In this time domain, we recover Eq. (6) of Ref. [27], and therefore have the same formal solution which, with the use of the quasineutrality condition, leads to

$$(\chi_{\mathrm{cl}} + \chi_{\mathrm{nc}})\phi_R(X) = \chi_{\mathrm{cl}}\phi(t = 0), \qquad (7)$$

where $\phi_R(X)$ is the time-asymptotic ($\omega_b t \gg 1$, but $t < \omega_{\mathrm{pr}}^{-1}$) value envelope of the residual vortex potential, and

$$\chi_{\mathrm{cl}} = \left\langle \int d^3v \frac{F_{i0}}{n_0} k_X^2\rho_i^2/2 \right\rangle = \langle k_X^2\rho_{Ti}^2 \rangle, \qquad (8)$$

$$\chi_{\mathrm{nc}} = \left\langle \int d^3v \frac{F_{i0}}{n_0}(Q_i - \bar{Q}_i)^2 \right\rangle, \qquad (9)$$

are classical and neoclassical susceptibilities in long-wavelength limit [35–37]. Here, $\langle\cdots\rangle$ is the flux surface average, ρ_{Ti} is the thermal ion Larmor radius, and $Q_i - \bar{Q}_i$

represents deviation of the guiding center from the bounce or transit orbit center of ions, shifted from the reference location by $\bar{Q}_i$. For fast ions, our long-wavelength approximations are not well justified and different asymptotic regimes should be considered. Effects of fast ions on the residual zonal flow have been addressed in the absence of MI showing a modest increase in the residual level [38]. In this calculation, we have considered an initial kick $N = -\delta(t)n_{pol}(t=0)/n_0$ [27] and neglected FLR and FOW of electrons, as they are much smaller than those of ions. Here, n_{pol} is the classical polarization density. Taking F_{i0} to be Maxwellian, with the use of polar coordinates [26], we obtain explicit expressions

$$\chi_{cl} = \{G_0(\rho) + G_1(\rho)\}k_w^2\rho_{Ti}^2, \tag{10}$$

$$\chi_{nc} = \{1.63G_0(\rho) + 0.12G_1(\rho)\}\frac{q^2}{\sqrt{\epsilon}}k_w^2\rho_{Ti}^2, \tag{11}$$

to the lowest order in the inverse aspect ratio $\epsilon = r/R$ and $\Delta_i\hat{s}/r_s$, where Δ_i is the ion orbit width. Here, $\rho \equiv \sqrt{(X+1)/2}$, $k_w \equiv 4S'(X)/w$ is a characteristic wave number of the vortex flow, and

$$G_0(\rho) \equiv \left\langle \frac{x^2}{w^2} \right\rangle = \frac{E(\rho)}{K(\rho)} - (1 - \rho^2), \tag{12}$$

and

$$G_1(\rho) \equiv \left\langle \frac{1}{4}\left(\frac{mw}{2r_s}\right)^2 \sin^2(m\alpha) \right\rangle$$
$$= \frac{1}{3}\left(\frac{mw}{2r_s}\right)^2 \left\{(2\rho^2 - 1)\frac{E(\rho)}{K(\rho)} + 1 - \rho^2\right\} \tag{13}$$

are the geometrical factors coming from the variation of the helical magnetic flux in radius r and helical angle α, respectively. The former is related to the finite magnetic shear $\hat{s}$, and the latter is due to the island perturbation $\delta\psi$. The factor $(mw/2r_s)^2$ in G_1 from $w^2 \sim \delta B_r \sim \delta\psi$ shows that G_1 represents the finite island width effect. In Eq. (11), note that while the magnetic drift in radius r yields the same enhancement factor as that of an axisymmetric tokamak [27], the drift in helical angle α results in an additional but subdominant contribution to the neoclassical polarization shielding. It is because the orbit tends to be distorted in a same way by the α component of the drift in the inner and the outer halves of the trajectory due to its even parity in θ, resulting in only a small effect on the orbit width.

From Eqs. (7)–(11), we obtain the residual vortex flow level

$$\frac{\phi_R}{\phi(t=0)} = \frac{\chi_{cl}}{\chi_{cl} + \chi_{nc}}$$
$$= 1 \bigg/ \left\{1 + \frac{1.63G_0(\rho) + 0.12G_1(\rho)}{G_0(\rho) + G_1(\rho)}\frac{q^2}{\sqrt{\epsilon}}\right\}, \tag{14}$$

for the timescale $\omega_{bi}^{-1} \ll t < \bar{\omega}_D^{-1}$. Because of the small numerical coefficient 0.12 for G_1 in the neoclassical susceptibility, this magnetic surface-dependent residual vortex flow level is comparable, but higher than the Rosenbluth-Hinton (RH) level [27] of the residual zonal flows in tokamaks. Obviously, the modification comes from the finite island width. So, the helically symmetric vortex is a robust structure in this timescale. Indeed, we recover the RH level in the limit of zero island width $mw/2r_s \to 0$, where $G_1 \to 0$. Figure 1 shows magnetic surface dependence of the residual vortex flow level. It is the highest at the O point and decreases continuously with ρ toward the island separatrix. In a cylindrical plasma, there is no magnetically trapped particles and no neoclassical enhancement of polarization shielding. Therefore the residual level in Eq. (14) approaches 1, as we take $\epsilon \to 0$ at fixed B_T/B_P.

In this Letter, we have neglected a magnetic field strength B inhomogeneity from the island perturbation $\delta\psi$ in the magnetic drift frequency $\omega_D = \mathbf{k} \cdot \mathbf{v}_d$, as its contribution to the magnetic drift velocity $\mathbf{v}_d \propto \mathbf{B} \times \nabla B$ (in low β) is smaller than that of toroicity by $\sim(w/r)^4\epsilon/q^2$. That is, the guiding center orbit has been approximated to be the same as that in the axisymmetric tokamak geometry and is thus governed by toroidicity. The MI effect on the residual vortex flow shown in Eq. (14) comes from the geometrical effect represented by ∇X in the vortex flow wave vector $\mathbf{k}$.
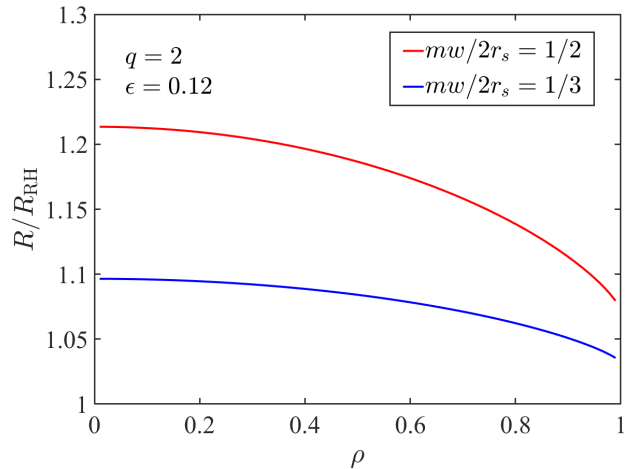
FIG. 1. Spatial dependence of the residual vortex flow level $R \equiv \phi_R/\phi(t=0)$ in a magnetic island with $mw/2r_s = 1/2$ (red) and $1/3$ (blue), for typical parameters $q = 2$ and $\epsilon = 0.12$ [39]. Here, we denote the Rosenbluth-Hinton residual level as $R_{RH} \equiv 1/(1 + 1.63q^2/\sqrt{\epsilon})$.

Long term evolution.—We continue our analysis in a longer time $\omega_{\mathrm{pr}}^{-1} < t$ using the same model for the source N. In the long term, the toroidal precession effect enters to the vortex flow dynamics. From Eq. (6), it is obvious that the toroidal precession breaks the helical symmetry and homogenizes the envelopes, which have been flux functions in X in a short term, along the tokamak magnetic surfaces ψ. This long term toroidicity-induced breaking of the helical symmetry of vortex flows is a reciprocal example of the RMP-induced long-term decay of zonal flows [40] in which a helical magnetic perturbation influences the axisymmetric zonal flow evolution. This shares a common physics with the zonal flow evolution in stellarators [41], that the long-term orbit deviation from the helical field structure results in a flow damping. The crucial difference is that while the secular radial drift of the helically trapped particles is the origin of the deviation in stellarators, it is the toroidal precession of the toroidally trapped particles which make the long-term effect in our problem. The equation for the final state after this homogenization is obtained using

$$\bar{\omega}_D = \omega_{\mathrm{pr}} \frac{\partial \Lambda}{\partial \zeta}\bigg|_\psi, \qquad (15)$$

a form exhibiting the proportionality $\bar{\omega}_D \propto \omega_{\mathrm{pr}}$. Hereafter, we assume a slowly varying $S'(X)$, and then we readily obtain $\Lambda = -S' \cos{(n\zeta)}$. From the functional similarity with the first term on the right-hand side (RHS) of Eq. (4), we realize that Λ represents finite magnetic surface deviation (FSD) from the tokamak surfaces due to the island perturbation. Multiplying Eq. (6) by $\exp{(i\Lambda)}$ and taking the drift average [42], we obtain the drift-averaged kinetic equation

$$\frac{\partial}{\partial t}[e^{i\Lambda} h](\psi) = \frac{e}{T} F_0[e^{i\Lambda}\overline{e^{iQ}J_0}\phi] + [e^{i\Lambda}\overline{e^{iQ}N}]F_0, \quad (16)$$

where $[\cdots] \equiv (\oint_d d\zeta(\cdots)/\omega_{\mathrm{pr}})/(\oint_d d\zeta/\omega_{\mathrm{pr}})$ is the drift average over the orbit center trajectory along the toroidal angle ζ. Now, the flow carried by the particles described in Eq. (16) is a mixture of the zonal and vortex flows

$$\delta\phi = \phi_M(\psi) \exp{\{iS(X)\}}. \qquad (17)$$

Here, a specific form ϕ_M is chosen to characterize the breaking of the helical symmetry due to the toroidal precession. Introducing X dependence in ϕ_M leads to a minor quantitative change, subdominant to that due to a fast variation in $\exp{\{iS(X)\}}$. We substitute the solution of Eq. (16) into the quasineutrality and take the flux surface average $\langle \cdots \rangle_0$ over the tokamak magnetic surface. Then, we obtain an expression of the envelope of the mixture ϕ_M

$$\langle e^{iS}\rangle_0 [1 - J_0^2(S')]\left(1 + \frac{T_i}{T_e}\right)\phi_M(\psi)$$
$$= J_0^2(S')\langle k_X^2 \rho_{Ti}^2 e^{iS}\phi(t=0)\rangle_0. \qquad (18)$$

In Eq. (18), $J_0(S')$ comes from the FSD factor $\exp(i\Lambda)$. Note that $\Lambda \lesssim 1$ is larger than the Larmor radius and orbit width $k_X \rho_i$ and Q for long-wavelength flows, which enables a simple expression of Eq. (18). Also, we have considered only the lowest-order orbits in an axisymmetric tokamaks for simplicity neglecting orbit modifications due to MI [43,44] which plays a role in MI evolution [32]. For a uniform initial vortex potential envelope $\phi(t=0)$, we have

$$\frac{\phi_M}{\phi(t=0)} = \frac{k_w^2 \rho_{Ti}^2}{1 + T_i/T_e}\frac{J_0^2(S')}{1 - J_0^2(S')}$$
$$\times \left[\frac{4x^2}{w^2} + \left(\frac{mw}{2r_s}\right)^2 \frac{J_0(S') + J_2(S')}{2J_0(S')}\right]. \qquad (19)$$

Note that there is a one-to-one correspondence between the radial distance x and the unperturbed poloidal magnetic flux ψ from the relation $d\psi = RB_\theta dr = (rB_\zeta/q)dr$. The amplitude of ϕ_M is smaller than ϕ_R in the interim state by $\sim k_w^2 \rho_{Ti}^2(1 + 1.6q^2/\sqrt{\epsilon})$, with an ordering $\phi_R \sim \phi_{\mathrm{RH}}$, $S' \sim 1$, and $J_0(S') \sim J_2(S') \sim 1$. Meanwhile, the inhomogeneity of the potential becomes more pronounced compared to that in the interim state. Accordingly, the mixture potential $\delta\phi$ in Eq. (17) is highly anisotropic on the island magnetic surfaces and forms localized E × B flow shear layers near the island separatrix, as shown in Fig. 2. In experiments, significant E_r shear has been observed near the island boundaries [13]. While such an E_r profile in the island region has typically been explained by the pressure profile modification, our result suggests a different origin of the localized E_r shear near the island separatrix.

We emphasize that the deviation of the potential contours, the streamlines of E × B flows, from the island magnetic surfaces effectively reduces the isolated region in an MI, changing from monopolar to dipolar vortex as shown in Fig. 2. The mixture flow tends to reduce the turbulence spreading [45] into an MI across its E × B flow shear layer [46] as with vortex flows [47]. However, turbulence can now move in-and-out of the MI across the island surfaces by an advection along the open streamlines near the X point.

In reality, this turbulence contamination could regulate slowly growing MIs. Indeed, for an example KSTAR discharge [39], $\bar{\omega}_D$ for the mixture formation is faster than the inverse resistive diffusion time $\eta/\mu_0 w^2$ characterizing the MI growth in the Rutherford regime [31]. The condition for a collisionless flow mixture presented in this Letter is $\bar{\omega}_D > \mu_\parallel k_\parallel^2$, where $\mu_\parallel$ is the parallel viscosity and $k_\parallel \sim (mw/2r_s)/(qR/\hat{s})$ is the parallel wave number of the mixture. For long mean free path tokamak plasmas [48], this leads to as $k_X \rho_{Ti} > \hat{s}/q$. With $S' \sim \mathcal{O}(1)$, this indicates
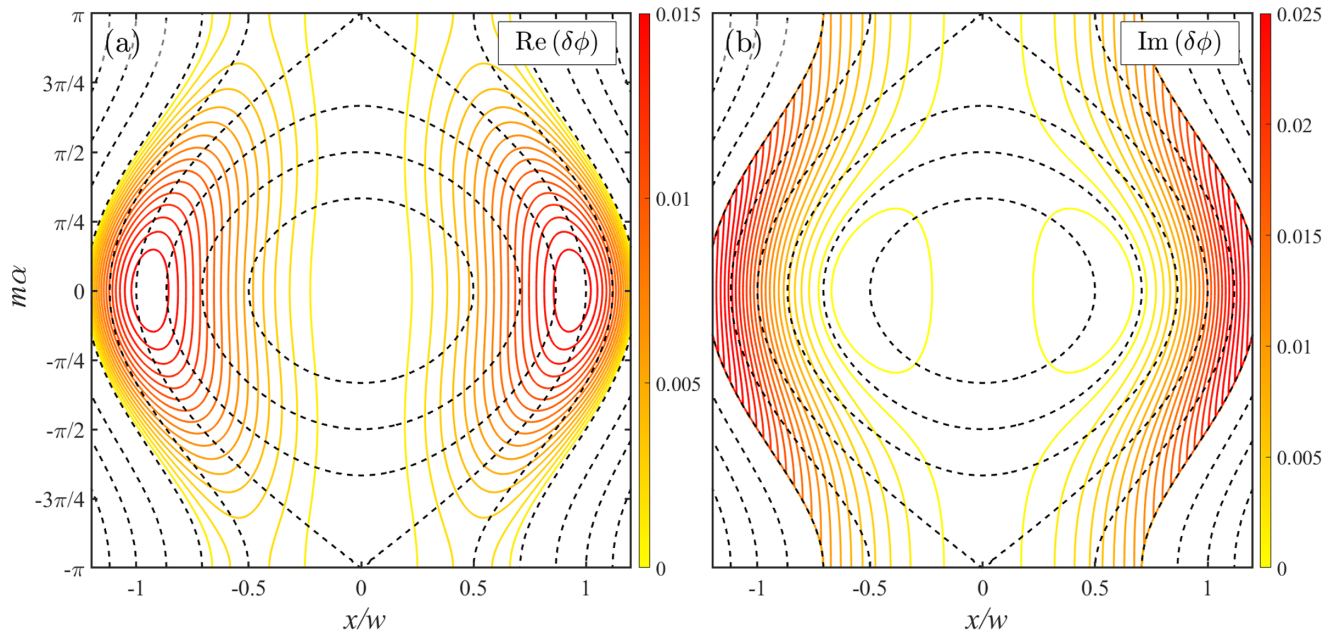
FIG. 2. Contour plots of the (a) real and (b) imaginary parts of the flow mixture potential $\delta\phi$ in the vicinity of a magnetic island, normalized by $\phi(t = 0)$, for a case of KSTAR discharge with a 2/1 tearing mode [39] having $mw/2r_s = 1/5$, $r_s = 25$ cm, $T_i \sim T_e \sim 0.4$ keV, and $B \sim 2$ T. The plot range is $-1 \leq X \leq 2$ and $S' = \pi/4$ as an example. The island contours have been plotted as black dashed lines.

that the flow mixture can be formed in a small MI with $w < q\rho_{Ti}/\hat{s}$. For a large MI with $w > q\rho_{Ti}/\hat{s}$, monopolar vortex would persist as reported in Ref. [16]. The $q/\hat{s}$ dependence of the critical island width can reconcile the result of Ref. [17], where a monopolar vortex was observed in an MI having smaller width in ρ_i unit than the critical size reported in Ref. [16].

Several issues, including the followings, remain to be addressed for a comprehensive description of turbulence-vortex flow interaction in an MI in tokamaks. Flow damping mechanisms other than linear collisionless damping studied in this Letter, such as collisional damping by neoclassical friction [49], nonlinear damping [50], and resonant potential vorticity diffusion [51], should be examined for vortex flows and flow mixtures. Also, works on the vortex flow generation considering toroidicity and island geometry are desired. In addition, the formalism employed in our work addressing the bounce-average and drift orbit of the bounce center in MI-distorted equilibrium can become useful in astrophysical systems such as particle acceleration in solar flares [52].

In summary, we have shown by gyrokinetic analyses that spatially dependent residual vortex flow level in a magnetic island is higher than the Rosenbluth-Hinton level due to finite island width, and that in a longer term, the residual vortex flows eventually evolve to the zonal-vortex flow mixtures by breaking of the helical symmetry by toroidal precession of flow-carrying particles. The mixture forms localized flow shear layers near the island separatrix away from the X points. At the same time, as the streamlines are detached from the magnetic surfaces, turbulence can be advected across the island along the mixture flow streamlines. Our results suggest new mechanisms of the $E \times B$ shear layer formation near the island boundaries and of the turbulence leakage into the island. Finally, we suggest different flow structure depending on the island size. We expect a dipolar flow mixture in a small island $w \lesssim q\rho_{Ti}/\hat{s}$, but a monopolar vortex flow in a large island $w \gtrsim q\rho_{Ti}/\hat{s}$.

*gyungjinc@snu.ac.kr

[1] A. Ishizawa, Y. Kishimoto, and Y. Nakamura, Plasma Phys. Controlled Fusion **61**, 054006 (2019).

[2] K. Ida, Plasma Phys. Controlled Fusion **62**, 014008 (2020).

[3] M. J. Choi, L. Bardóczi, J.-M. Kwon, T. S. Hahm, H. K. Park, J. Kim, M. Woo, B.-H. Park, G. S. Yun, E. Yoon, and G. McKee, Nat. Commun. **12**, 375 (2021).

[4] H. P. Furth, J. Killeen, and M. N. Rosenbluth, Phys. Fluids **6**, 459 (1963).

[5] T. S. Hahm and R. M. Kulsrud, Phys. Fluids **28**, 2412 (1985).

[6] R. Fitzpatrick, Nucl. Fusion **33**, 1049 (1993).

[7] R. Nazikian, C. Paz-Soldan, J. D. Callen, J. S. deGrassie, D. Eldon et al., Phys. Rev. Lett. **114**, 105002 (2015).

[8] T. E. Evans, R. A. Moyer, P. R. Thomas, J. G. Watkins, T. H. Osborne *et al.*, Phys. Rev. Lett. **92**, 235003 (2004).

[9] K. Ida *et al.*, Phys. Plasmas **11**, 2551 (2004).

[10] K. H. Burrell, Phys. Plasmas **4**, 1499 (1997).

[11] T. S. Hahm, Plasma Phys. Controlled Fusion **44**, A87 (2002).

[12] K. Ida *et al.*, Nucl. Fusion **44**, 290 (2004).

[13] T. Estrada, E. Ascasíbar, E. Blanco, A. Cappa, C. Hidalgo, K. Ida, A. López-Fraguas, and B. Ph van Milligen, Nucl. Fusion **56**, 026011 (2016).

[14] A. Ishizawa and N. Nakajima, Nucl. Fusion **49**, 055015 (2009).

[15] W. A. Hornsby, A. G. Peeters, A. P. Snodin, F. J. Casson, Y. Camenen, G. Szepesi, M. Siccinio, and E. Poli, Phys. Plasmas **17**, 092301 (2010).

[16] A. Bañón Navarro, L. Bardóczi, T. A. Carter, F. Jenko, and T. L. Rhodes, Plasma Phys. Controlled Fusion **59**, 034004 (2017).

[17] K. S. Fang and Z. Lin, Phys. Plasmas **26**, 052510 (2019).

[18] Z. Lin, T. S. Hahm, W. W. Lee, W. M. Tang, and R. B. White, Science **281**, 1835 (1998).

[19] P. H Diamond, S.-I. Itoh, K. Itoh, and T. S. Hahm, Plasma Phys. Controlled Fusion **47**, R35 (2005).

[20] L. Schmitz, Nucl. Fusion **57**, 025003 (2017).

[21] A. Hasegawa and M. Wakatani, Phys. Rev. Lett. **59**, 1581 (1987).

[22] K. H. Burrell, Phys. Plasmas **27**, 060501 (2020).

[23] M. Jiang *et al.*, Nucl. Fusion **59**, 046003 (2019).

[24] J.-M. Kwon, S. Ku, M. J. Choi, C. S. Chang, R. Hager, E. S. Yoon, H. H. Lee, and H. S. Kim, Phys. Plasmas **25**, 052506 (2018).

[25] C. J. McDevitt and P. H. Diamond, Phys. Plasmas **13**, 032302 (2006).

[26] T. S. Hahm, Y. J. Kim, P. H. Diamond, and G. J. Choi, Phys. Plasmas **28**, 022302 (2021).

[27] M. N. Rosenbluth and F. L. Hinton, Phys. Rev. Lett. **80**, 724 (1998).

[28] E. A. Frieman and L. Chen, Phys. Fluids **25**, 502 (1982).

[29] T. S. Hahm, Phys. Fluids **31**, 2670 (1988).

[30] A. J. Brizard and T. S. Hahm, Rev. Mod. Phys. **79**, 421 (2007).

[31] P. H. Rutherford, Phys. Fluids **16**, 1903 (1973).

[32] H. R. Wilson, J. W. Connor, R. J. Hastie, and C. C. Hegna, Phys. Plasmas **3**, 248 (1996).

[33] R. D. Hazeltine and J. D. Meiss, *Plasma Confinement* (Dover Publications, New York, 2003), Reprint edition.

[34] P. Helander, A. Mishchenko, R. Kleiber, and P. Xanthopoulos, Plasma Phys. Controlled Fusion **53**, 054006 (2011).

[35] Y. Xiao and P. J. Catto, Phys. Plasmas **13**, 102311 (2006).

[36] L. Wang and T. S. Hahm, Phys. Plasmas **16**, 062309 (2009).

[37] F.-X. Duthoit, A. J. Brizard, and T. S. Hahm, Phys. Plasmas **21**, 122510 (2014).

[38] Y. W. Cho and T. S. Hahm, Nucl. Fusion **59**, 066026 (2019).

[39] M. J. Choi *et al.*, Nucl. Fusion **57**, 126058 (2017).

[40] G. J. Choi and T. S. Hahm, Nucl. Fusion **58**, 026001 (2018).

[41] H. Sugama and T.-H. Watanabe, Phys. Plasmas **13**, 012501 (2006).

[42] J. R. Cary and A. J. Brizard, Rev. Mod. Phys. **81**, 693 (2009).

[43] K. Imada, H. R. Wilson, J. W. Connor, A. V. Dudkovskaia, and P. Hill, Phys. Rev. Lett. **121**, 175001 (2018).

[44] A. V. Dudkovskaia, J. W. Connor, D. Dickinson, P. Hill, K. Imada, S. Leigh, and H. R. Wilson, Plasma Phys. Controlled Fusion **63**, 054001 (2021).

[45] T. S. Hahm and P. H. Diamond, J. Korean Phys. Soc. **73**, 747 (2018).

[46] W. X. Wang, T. S. Hahm, W. W. Lee, G. Rewoldt, J. Manickam, and W. M. Tang, Phys. Plasmas **14**, 072306 (2007).

[47] K. Ida, T. Kobayashi, M. Ono, T. E. Evans, G. R. McKee, and M. E. Austin, Phys. Rev. Lett. **120**, 245001 (2018).

[48] R. Fitzpatrick, Phys. Plasmas **2**, 825 (1995).

[49] F. L. Hinton and M. N. Rosenbluth, Plasma Phys. Controlled Fusion **41**, A653 (1999).

[50] E.-J. Kim and P. H. Diamond, Phys. Plasmas **9**, 4530 (2002).

[51] J. C. Li and P. H. Diamond, Phys. Plasmas **25**, 042113 (2018).

[52] S. Tsuneta, Publ. Astron. Soc. Jpn. **47**, 691 (1995).